Carbohydrate Polymers 93 (2013) 291–299

Contents lists available at SciVerse ScienceDirect

Carbohydrate Polymers

journal homepage: www.elsevier.com/locate/carbpol

Physicochemical design of the morphology and ultrastructure of cellulose beads

Jani Trygg[a,*], Pedro Fardim[a], Martin Gericke[a], Ermei Mäkilä[b], Jarno Salonen[b]

[a] Åbo Akademi, Laboratory of Fibre and Cellulose Technology, Finland[1]
[b] University of Turku, Department of Physics, Laboratory of Industrial Physics, Finland

ARTICLE INFO

Article history:
Received 4 January 2012
Received in revised form 21 March 2012
Accepted 27 March 2012
Available online 5 April 2012

Keywords:
Cellulose beads
Dissolution
Coagulation
NaOH–urea
Structure design

ABSTRACT

Cellulose was dissolved in NaOH–urea–water and beads were prepared by coagulation into nitric acid as well as saline solution. Morphology and ultrastructure of the beads were modified by controlling the molarity of the acid (0–10 M) and temperature (5–50 °C) of the coagulation media and the cellulose concentration (3–7%). The beads were characterized by optical image analysis (shape, volume, and size distribution) and weight (total porosity). Cross-sections of CO_2 critical point dried beads were studied by field emission scanning electron microscopy (FE-SEM) and specific surface areas of 336–470 $m^2\,g^{-1}$ were determined from nitrogen adsorption isoterms. Pore size distribution was analyzed using solute exclusion technique. Our results demonstrate that the ultrastructure can be controlled by alteration of the coagulation conditions. Changes in size, shape and surface area were substential. Also generation of micro- ($\leqslant$2 Å), meso-, or macropores ($\geqslant$50 Å) can be favored.

1. Introduction

Cellulose gained increasing interest in research due to its attractive properties, such as abundance, biodegradability, and renewability. The polysaccharide can be chemically modified in different ways to obtain derivatives with specific properties, ranging from hydrophilic to hydrophobic, from non-charged to an-, or cationic (Heinze, Liebert, & Koschella, 2006; Klemm, Philipp, Heinze, Heinze, & Wagenknecht, 1998). Moreover, cellulose can be shaped into well defined objects such as fibers of different geometry, films, sponges, or spherical particles that are also known as cellulose beads (Gavillon & Budtova, 2008; Lönnberg, 2005).

Cellulose beads are versatile materials for numerous applications, especially when they have been chemically modified in order to support their performance. They are excellent filling materials for chromatographic columns because they can withstand high flow rates due to the spherical shape (De Oliveira & Glasser, 1996; Kaster, de Oliveira, Glasser, & Velander, 1993). Thus, cellulose beads could be employed as stationary phase for size exclusion chromatography and as selective adsorbents for biological substances such as proteins, endotoxins, and viruses (De Oliveira & Glasser, 1996; Xia, Lin, Wang, Chen, & Yao, 2008; Yamamoto & Miyagawa, 1999). Ionic cellulose beads found use in ion-exchange and water treatment (Hirota, Tamura, Saito, & Isogai, 2009). Also pharmaceutical applications have been reported. Cellulose beads could be loaded with drugs that are gradually released from these materials afterwards (Volkert, Wolf, Fischer, Li, & Lou, 2009; Wolf, 1997).

In general, preparation of cellulose beads involves three steps: dissolution, shaping, and regeneration of the polysaccharide. Different procedures have been developed, mainly differing in the solvent applied and the technique utilized to obtain spherical particles. Cellulose beads have be prepared for instance by dropping (De Oliveira & Glasser, 1996), jet cutting (Pinnow, Fink, Fanter, & Kunze, 2008), spinning drop atomization (Rosenberg, Suominen, Rom, Janicki, & Fardim, 2007), spraying (Chen & Tsao, 1976) and dispersion (Luo & Zhang, 2010; Motozato & Hirayama, 1984; Peška, Štamberg, & Hradil, 1976). Many different solvents for the dissolution, shaping, and chemical derivatization of cellulose have been reported (Liebert, Heinze, & Edgar, 2010). Nevertheless, cellulose beads have been mostly prepared, via one of the above described techniques, by exploiting the viscose process or by utilizing organosoluble cellulose acetates as a starting material (Štamberg, Peška, Paul, & Philipp, 1979; Motozato & Ishibashi, 1981; Rosenberg et al., 2007; Thümmler et al., 2011). Although both processes have been brought to commercial applications, they show several disadvantages that hamper the utilization of cellulose beads (Motozato & Ishibashi, 1981; Peška, Štamberg, & Blace, 1977). Cellulose is temporary converted into a more or less stable derivative. The substituent, rendering the polysaccharide soluble, is first introduced and finally removed again from the final material, which is inefficient and implies the use of excess chemicals and the

* Corresponding author. Current address: Åbo Akademi, Fibre and Cellulose Technology, Porthansgatan 3, 20500 Turku, Finland.
E-mail address: jtrygg@abo.fi (J. Trygg).
[1] Member of the European Polysaccharide Network of Excellence (EPNOE), http://www.epnoe.eu.

0144-8617/$ – see front matter © 2012 Elsevier Ltd. All rights reserved.
http://dx.doi.org/10.1016/j.carbpol.2012.03.085

production of additional waste. In addition, the use of toxic CS_2 in the viscose process raises considerable environmental and safety issues.

Utilization of non-derivatizing and environmental friendly solvents is a more convenient approach for shaping of cellulose. Aqueous systems such as NaOH–water, NaOH–urea–water and NaOH–ZnO–water have raised a lot of interest for this purpose (Egal, Budtova, & Navard, 2008; Jin, Zha, & Gu, 2007; Liu, Budtova, & Navard, 2011; Zhang, Ruan, & Gao, 2002). Preparation of cellulose beads from these novel solvents has been reported as well using either dispersion or dropping techniques (Luo & Zhang, 2010; Rosenberg, Rom, Janicki, & Fardim, 2008; Sescousse, Gavillon, & Budtova, 2011). Later are of particular interest because they enable preparation of comparably large beads (from several 100 μm up to 1–2 mm) in large batches, if sophisticated technical devices such as spinning drop atomization are applied.

In the present comprehensive study, cellulose beads were prepared from NaOH–urea–water solution via dropping technique. The aim was to understand the influence of different preparation parameters on the macroscopic (e.g., size, shape, and density) and microscopic (e.g., inner morphology and pore size distribution) bead properties. Studying ways to control these parameters is vital for any application, novel as well as already established ones, since they determine the performance of the cellulose beads. Based on the gained result it is possible to obtain tailored materials that may be utilized in different areas.

2. Experimental

2.1. Materials

Dissolving pulp (Cellulose plus) was purchased from Domsjö Fabriker, Sweden. The pulp had a α-cellulose content of 93% and contained 0.6% of lignin (Domsjö, 2007). Intrinsic viscosity of the delivered pulp was reported to be $530 \pm 30\,cm^3g^{-1}$ according to SCAN-CM 15:99 standard after two stage sodium based cooking. Pulp was Total Chlorine Free (TCF)-bleached. Urea (99.5%) and nitric acid (65%) were purchased from Merck KGaA, NaCl (100.0%) and acetone (99.5%) from J.T. Baker, and NaOH (97%) from Fluka Analytical. Dextrans were purchased from Sigma–Aldrich and used as received.

2.2. Pretreatment of the pulp

The Pulp was pretreated in ethanol-hydrochloric acid for 2 h at 75 °C as described earlier (Trygg & Fardim, 2011). Intrinsic viscosity of the pretreated pulp was measured according to standard ISO/FDIS 5351:2009 and viscosity average degree of polymerization was calculated (Immergut, Schurz, & Mark, 1953). 0.2 M cuprietylene-diamine (CED) solution was dropped on the pretreated pulp fibres and optical microscopy was used to detect any ballooning (Cuissinat & Navard, 2006). The Pulp was dried in an oven at 60 °C overnight and stored at room temperature.

2.3. Dissolution of cellulose in NaOH–urea–water

Pretreated pulp was mixed with a solution of 7% NaOH and 12% urea in water so that the dry content of cellulose was 4%, 5% or 6% from the total weight of the final solution. Humidity of the pulp varied between 2% and 7% and this was included in the amount of water in solution. After 10 min of vigorous stirring the suspension of pulp and solvent was cooled to −10 °C and stirring was continued for half an hour. The solution became visually transparent approximately in 15 min from the beginning of the cooling.

2.4. The determination of gelation times

Gelation times of the 4–6% cellulose in NaOH–urea–water solution were determined using an Anton Paar Physica MCR 300 rotational rheometer with DG 26.7 double-gap cylinder. Temperature was set to 20 and 25 °C with a TEZ 150P thermostat with external water cycle. G' and G'' were measured with amplitude of 1% and frequency of 1 rad/s and gelation times were taken from the crossing point of both moduli.

2.5. Preparation of cellulose beads

Cellulose solutions were directly taken from the cooling device (−10 °C) and extruded through Eppendorf 5 ml syringe tip into the coagulation solutions. Height of the tip was manually adjusted in situ 1–2 cm above the surface to gain as spherical beads as possible. Beads were prepared in beakers of the same geometry (1 dm^3, ∅ 11.5 cm) in order to exclude possible effects due to changes of the surface tension of the coagulation media, sinking height, etc. Stirring was applied only occasionally to even concentration gradients. Each coagulation experiment took less than 10 min, which is notably shorter than gelation times of cellulose solutions (see Section 3.1).

Temperature, cellulose content, and concentration of the coagulation media were varied separately while keeping the other variables constant. Concentration of cellulose was 5% from the total weight of the solution, unless otherwise mentioned. Since cellulose solution is highly alkaline, high volumes of the acidic coagulation media was used in order to minimize the neutralization. Maximum allowed change was 0.5 M of the initial acid concentration except for the 0.5 M nitric acid solution where the change was 0.1 M. When coagulating in 10% NaCl solution, the final NaOH concentration did not exceeded 0.35 M.

Effect of the temperature of the coagulation media was studied with 2 M nitric acid solution and 10% NaCl solution at 5, 25 and 50 °C. Beads coagulated at 5 and 25 °C were kept at that temperature for the whole coagulation time and beads coagulated at 50 °C were kept at that temperature for 2 h and then cooled to 25 °C.

Effect of the acid concentration on the coagulation of the cellulose solution was studied with 0.5, 2, 4, 6, 8 and 10 M nitric acid at 25 °C. 2 M nitric acid at 25 °C was also used to coagulate 4% and 6% cellulose solutions.

Coagulated beads were left in acid overnight and in saline water for two nights. After one night the saline water was changed. All the beads were washed under running tap water for 30 min, distilled water for 15 min and stored in distilled water at room temperature for further use.

2.6. Critical point drying

In order to study the surface area of the beads and their structure (see Sections 2.7 and 2.8), water was exchanged to acetone by a step-wise procedure and beads were critical point dried with a Critical Point Dryer (Balzers Union Limited, Liechtenstein) using liquid CO_2 to maintain the porous structure. Some beads were cut half before being critical point dried (CPD).

2.7. Field emission scanning electron microscopy

Interior, edge, and surface morphology of the coagulated cellulose CPD beads were examined using a Leo Gemini 1530 field emission scanning electron microscope (FE-SEM) with a In-Lens detector. The whole beads as well as their cross-sections were coated with carbon in Temcarb TB500 sputter coater (Emscope Laboratories, Ashfold, UK). An optimum accelerating voltage for

Table 1
Molar masses and diameters of dextrans in solution used in solute exclusion technique.

Molecule	Molar mass (g mol^{-1})	Size (Å)
Dextrans	6k	39
	40k	91
	100k	139
	500k	290
	2000k	560

FE-SEM was 5.00 kV and magnifications were between 250× and 10,000×.

2.8. Specific surface area

Nitrogen adsorption measurements at 77 K were performed with CPD-beads with TriStar 3000 gas sorption apparatus (Micromeritics, Norcross, USA). The specific surface area of the beads was determined from the obtained adsorption isotherm using the equation by Brunauer, Emmett and Teller (BET equation) (Brunauer, Emmett, & Teller, 1938).

2.9. Determination of size, shape, and weight

Effect of the coagulation condition on the size distribution, average size, and shape were studied by taking images of 20–100 paper dried (wet) beads and beads that were dried in an oven at 105 °C overnight (dry). In addition, weight of the beads was determined in each case. Minimum 20 beads were used to calculate the average weight.

Optical images were converted to binary images, shapes were fitted to ellipse, and shape descriptors (minor and major axis, circularity) were computed using Fiji image processing software (Schindelin, 2008). Volumes of the beads were calculated using the length of the minor axis assuming full sphericity. Size distributions were normalized and Gaussian fit was used to determine the peak center and full width at half maximum (FWHM). Total porosity was calculated from the wet and dry weights of the beads and using density 1.5 g cm^{-3} for bulk cellulose (Ettenauer et al., 2011).

2.10. Solute exclusion technique

Accessibility of macromolecules into the pores of the beads was analyzed by solute exclusion technique. Molecular diameter of the macromolecules was interpolated from the literature values (Stone & Scallan, 1968). Molecular masses and sizes in solution are listed in Table 1.

Since the removal of the surplus water was found challenging and accuracy was unreproducible, method in literature (Ettenauer et al., 2011; Stone & Scallan, 1967, 1968) was modified. Approximately 4 g of wet beads were sunken in water so that total weight was accurately weighed to be 5 g. Precisely 5 g of 6% dextran solution were pipetted into the mixture and gentle stirring was applied for few hours. Concentration of the macromolecules and calibration solutions was measured using Perkin-Elmer 241 Polarimeter with Na-lamp radiation source (589 nm), readout accuracy 0.001°. After solute exclusion, beads were washed with excess water, left in distilled water for few hours, filtered, and dried in an oven at 105 °C overnight. The Filtrate was used to follow the washing performance and the remaining of macromolecules in water.

Beads were dried overnight at 105 °C and dry weigh was measured. Inaccessible water of the pores, i.e. water in small pores where macromolecules cannot access, was calculated using the equation:

$$\text{Inaccessible water} = m_{\text{water+beads}} - m_{\text{dry beads}} + m_{\text{solute}} - \frac{m_{\text{solute}} \cdot c_{\text{solute},0}}{c_{\text{solute},f}} \quad (1)$$

where $m_{\text{water+beads}}$ is total weigh of wet beads and water, m_{drybeads} the dry weight of the beads, m_{solute} the weight of the 6% macromolecule solution added into the mixture, $c_{\text{solute},0}$ the initial concentration of the macromolecules and $c_{\text{solute},f}$ the final measured concentration of the macromolecules. Inaccessible water in beads is located in pores which are too small for macromolecules to access. Total accessible water and saturation point for macromolecules was computed using non-linear curve fitting (logistic model) of Origin Software (2002). Frequency of pores was calculated using the equation:

$$\text{Frequency} = \frac{\text{Total accessible water} - \textit{Inaccessible} \text{ water}}{\text{Total accessible water}} \quad (2)$$

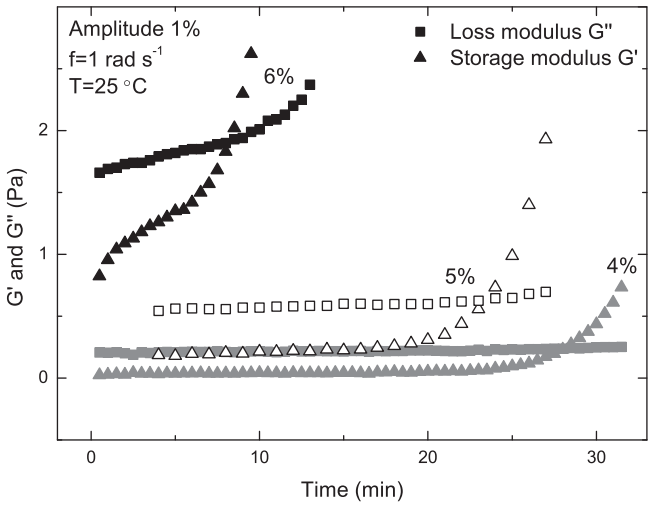

Fig. 1. Storage and loss moduli of cellulose solutions in 7% NaOH–12% urea–water at 25 °C.

3. Results and discussion

3.1. Preparation and stability of cellulose solutions

Intrinsic viscosity of ethanol-acid pretreated pulp was measured and viscosity average degree of polymerization (DP_v) was calculated to be 173. Practically the same value (174) was reported earlier (Trygg & Fardim, 2011). Ballooning was not observed in 0.2 M CED solution indicating the absence of the primary cell wall layer.

Washed and dried pulp was dispersed in NaOH–urea–water solution, cooled to −10 °C and dissolved. Gelation times were determined from the crossing points of storage and loss modulus of rheological measurements of visually transparent solutions (Fig. 1). For 6% cellulose solution 25 °C gelation occurred after 8 min which is notably shorter than for 4% (28 min) and 5% (23 min) solutions (Table 2). At 20 °C gelation time for 6% solution was over 33 min. Since the solutions were not heated after taking them from the −10 °C cooling device and coagulation procedure did not take more than 10 min, the temperature of the solutions remained cooler than 20 °C. Gelation of the solutions was not observed during the coagulation of the beads.

Table 2
Gelation times of cellulose solutions in 7% NaOH–12% urea–water at 25 °C with amplitude of 1% and frequency of 1 rad s^{-1}.

Cellulose concentration (%)	Gelation time (min)
4%	28.1
5%	23.5
6%	8.2
6%[a]	33.4

[a] 20 °C.

Table 3
Gaussian parameters of normalized size distribution values from images of cellulose beads prepared under different conditions.

Preparation conditions			Gaussian parameters	
$c_{cellulose}$ (%)	T (°C)	c_{HNO_3} (M)	Peak (mm)	FWHM[a]
4	25	2	2.92	0.16
5	25	2	2.97	0.16
6	25	2	2.99	0.20
5	25	0.5	2.71	0.32
5	25	2	2.97	0.16
5	25	4	2.67	0.60
5	25	6	3.02	0.58
5	25	8	3.05	0.27
5	25	10	3.31	0.41
5	5	2	2.41	0.37
5	25	2	2.70	0.24
5	50	2	2.85	0.21
5	5	[b]	2.79	0.32
5	25	[b]	2.76	0.24
5	50	[b]	3.20	0.14

[a] Full width at half maximum.
[b] 10% NaCl was used instead of HNO_3.

3.2. Tailoring of size distribution, size, shape and weight

The effect of cellulose concentration in NaOH–urea–water as well as the coagulation bath conditions (medium, temperature and concentration) was studied by optical image analysis and weight. Only one variable was studied at a time and the others were kept constant. Measured parameters were volume, circularity, porosity and mass. Also size distribution values were calculated. The drop height of the cellulose solutions into the coagulation medium was observed to have significant effect on the bead shape. Most spherical beads, i.e. ones having circularity close to 1, were produced when the tip of the pipette was 1–2 cm from the surface of the coagulation medium.

Volume and weight were observed to increase with increasing temperature (Fig. 2A, upper) for nitric acid and saline water. At higher temperature, coagulation happened faster than at lower temperatures. This caused the skin layer to become firm faster and dimensions of the droplet were preserved. It is reasonable that at lower temperatures slower coagulation packed cellulose molecules more densely and proceeding coagulation inside of the skin layer pulled outer layers closer and caused slight shrinking of the bead. Changes were observed also in size distribution values (Table 3). When temperature increased, peak values increased and distributions narrowed. Since bigger beads can hold more water inside, weight increased with volume. Because volume and weight increased simultaneously, porosity values changed relatively little (Fig. 2A, lower). However, decrease in porosity at 5–25 °C can be seen, followed by increase at 50 °C. This indicates higher proportion of micro- and small mesoropores at 25 °C and macropores at 50 °C.

Circularity was noted to be highly influenced by the temperature of the coagulation medium (Fig. 2A, lower). Circularity increased from 0.755 to 0.892 (HNO_3) and from 0.687 to 0.823 (10% NaCl) when temperature increased from 5 to 50 °C. At lower temperatures tails were formed because coagulation kinetic is low and shear forces of the falling droplet relatively high, which explains the decreased fit to ellipse (lower circularity).

When concentration of nitric acid was increased from 2 M to 8 M, volume did not change (Fig. 2B, upper). However, 0.5 M acid yielded notably smaller and 10 M acid bigger beads. Weight values are following the same trend, with exception of weight of the beads coagulated into 4 and 6 M acids. This can be explained by the wide size distribution values (Table 3, FWHW for 4 and 6 M) and hence fluctuation in volume and weight values.

Circularity did not change much with increasing acid concentration. Beads took their form soon after the contact with acid and tail formation was minimal during the fall of the droplet. Porosity values increased when acid concentration was increased from 0.5 to 8 M. Beads coagulated into 10 M acid had clearly lower porosity. This might be due to changed coagulation mechanism (see Section 3.3). Increase in porosity indicates that more macropores are present.

Cellulose concentration in NaOH–urea–water had a small effect on volume and weight (Fig. 2C, upper). Beads were coagulated into 2 M acid at 25 °C, which caused rapid formation of the skin layer. Since the dimensions did not change much, also changes in weight and size distribution parameters were small (Table 3). Peak values did not change and width of the distribution was narrow for all cellulose concentrations, 6% being slightly wider than others. Cellulose concentration had very little effect on circularity (Fig. 2C, lower). A small decrease was seen in circularity when concentration was 6%. This is due to higher viscosity and tail formation when the droplet leaves the tip. However, porosity decreased with increasing cellulose concentration (Fig. 2C, lower). Since the constant volume was filled with more cellulose, apparent density of cellulose was founded to be higher. With low cellulose concentration same volume is filled with more voids. When cellulose concentration was further decreased to 3%, beads did not hold together anymore. On the other hand, cellulose solutions with concentrations above 6% were too viscous to extrude through the tip of the pipette without forming a continuous flow.

3.3. Morphological changes

Morphological changes of CPD cellulose beads were studied with FE-SEM. Beads were coagulated into nitric acid with different molarities at 25 °C using 5% cellulose solution. Also 4% and 6% cellulose solutions were coagulated into 2 M nitric acid at 25 °C in order to study the effect of the cellulose concentration.

Surface of the CPD beads, coagulated into 0.5 M nitric acid, was more coarse than that of beads, coagulated into more concentrated acid (Fig. 3). The fact that wider cavities and cellulose fibrils (aggregates) cannot be seen on the surface indicates that aggregation continued to form more solid structures after the first contact with acid, or that coagulation proceeded via other mechanism. Faster coagulation in 2, 6 and 10 M acids intercepted the aggregation of the cellulose fibrils and resulted fine structures with cavities (Fig. 3B–D). Coagulation in 10 M acid produced notably smaller cavities between fibrils than in 2 and 6 M acid. It is possible that due to shortened coagulation time fibrils did not have time to merge and fibril size decreased. In cross-section images, a small skin-core structure could be observed when the concentration of the coagulation acid was higher than 0.5 M (Fig. 4). Significant differences between skin thickness was not observed between 2 and 6 M coagulation media (~3–6 μm) but coagulation into 10 M acid caused considerably thicker skin layer (~50 μm). During the coagulation in 10 M acid nucleation centers on the surface of the droplets were observed, whereas in lower concentrations coagulation proceeded simultaneously along the surface. In FE-SEM images, plate-like

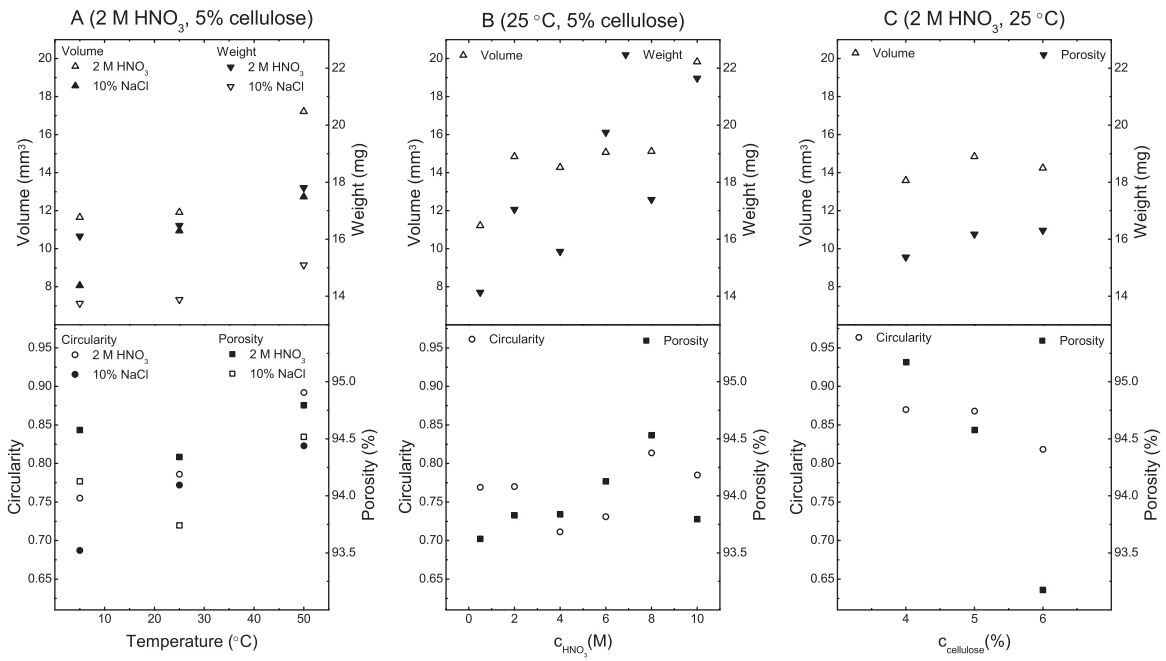

Fig. 2. The effect of (A) temperature, (B) acid concentration, and (C) cellulose concentration on volume (△, ▲), weight (▼, ▽), circularity (○, ●) and porosity (■, □). Constant parameters are given above the figures.

structures were seen (Fig. 4D), supporting a competing coagulation mechanism when stronger acid was used. Differences in the interior parts of the cross-sections were also studied. Coagulation into 0.5 and 2 M acid produced bigger agglomerates and less smooth surfaces inside of the bead compared to 6 and 10 M acid (Fig. 5). As mentioned above, fibrils continued to merge on the surface even after the contact with acid when concentration was low. Since the coagulation inside of the bead is more diffusion controlled and slower than on the surface, beads coagulated in 2 M acid could produce larger agglomerates. However, higher acid concentration intercepted the aggregation and hence resulted thinner fibrils and finer structures. In addition, beads coagulated into 8 and 10 M acid were weaker and could be flattened easily under pressure. When 4% and 6% cellulose solutions were coagulated in 2 M acid at 25 °C, morphology of the surfaces was similar as seen for 5% solution (Fig. 6). Skin-core structures were observed for both

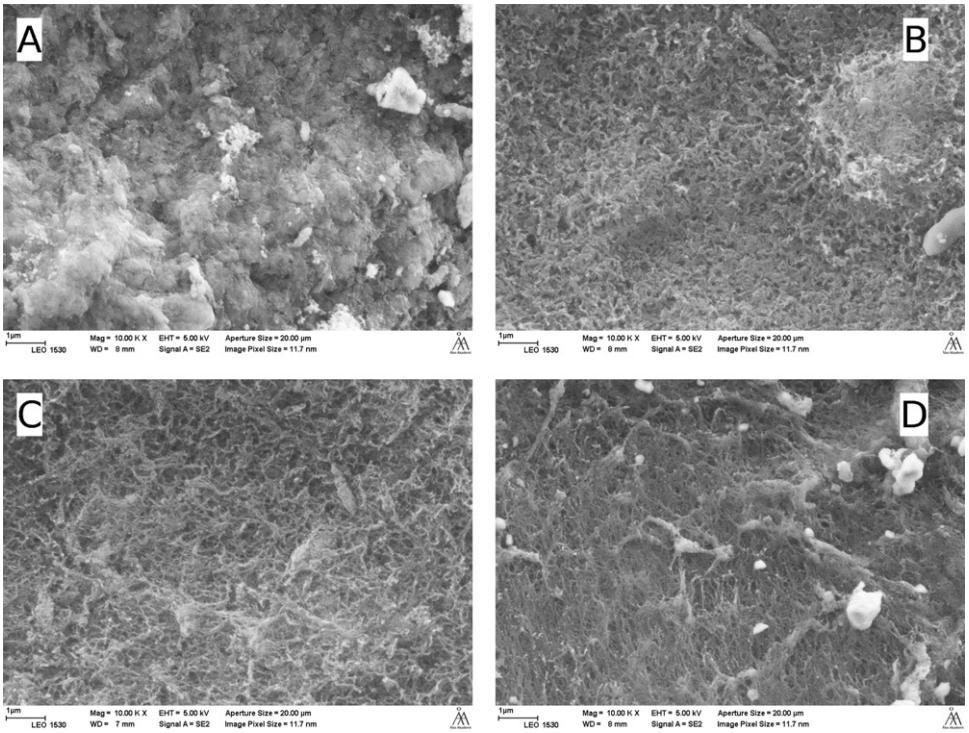

Fig. 3. FE-SEM images of the surface of CPD cellulose beads. 5% cellulose solution was coagulated into (A) 0.5 M, (B) 2 M, (C) 6 M and (D) 10 M HNO_3 at 25 °C. Magnification is 10,000×.

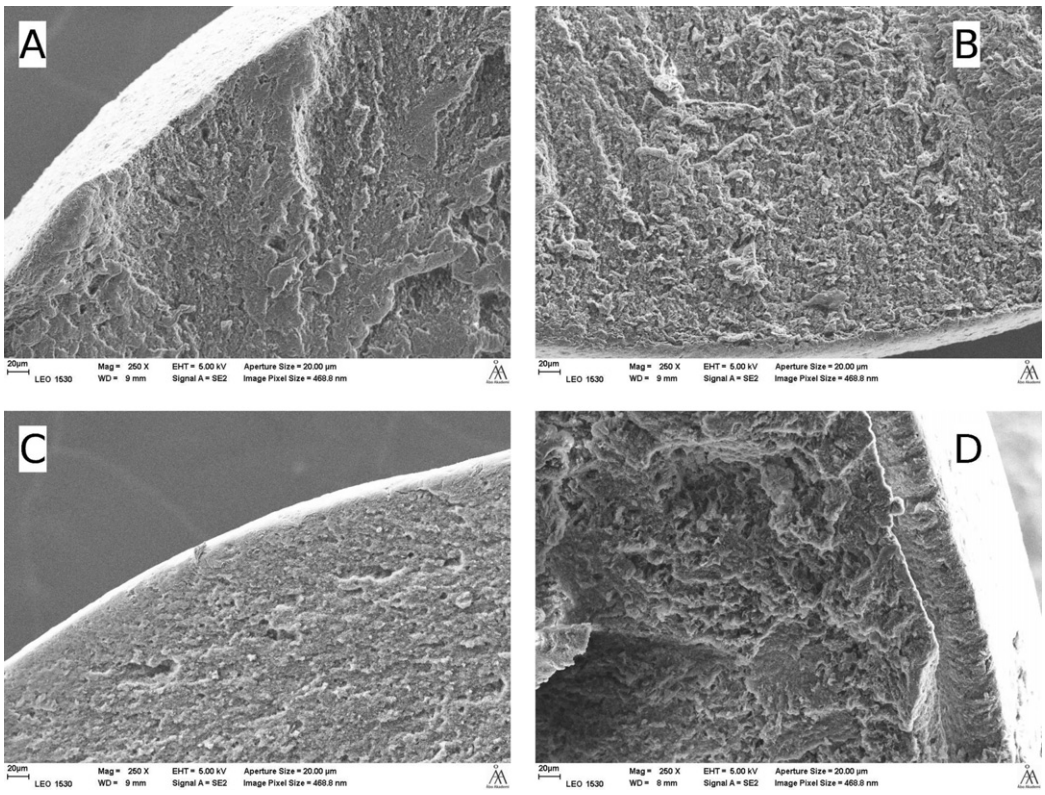

Fig. 4. FE-SEM images of the cross-sections of CPD cellulose beads. 5% cellulose solution was coagulated into (A) 0.5 M, (B) 2 M, (C) 6 M and (D) 10 M HNO_3 at 25 °C. Magnification is 250×.

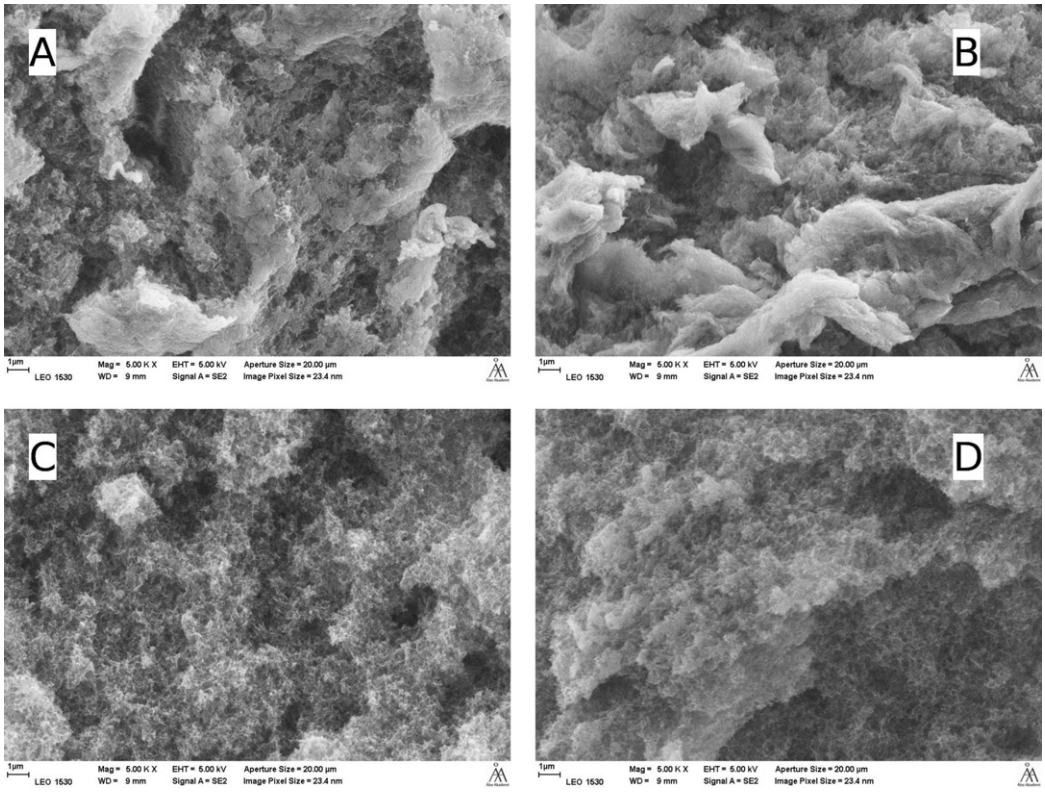

Fig. 5. FE-SEM images of the interior of the cross-sections of the CPD cellulose beads. 5% cellulose solution was coagulated into (A) 0.5 M, (B) 2 M, (C) 6 M and (D) 10 M HNO_3 at 25 °C. Magnification is 10,000×.

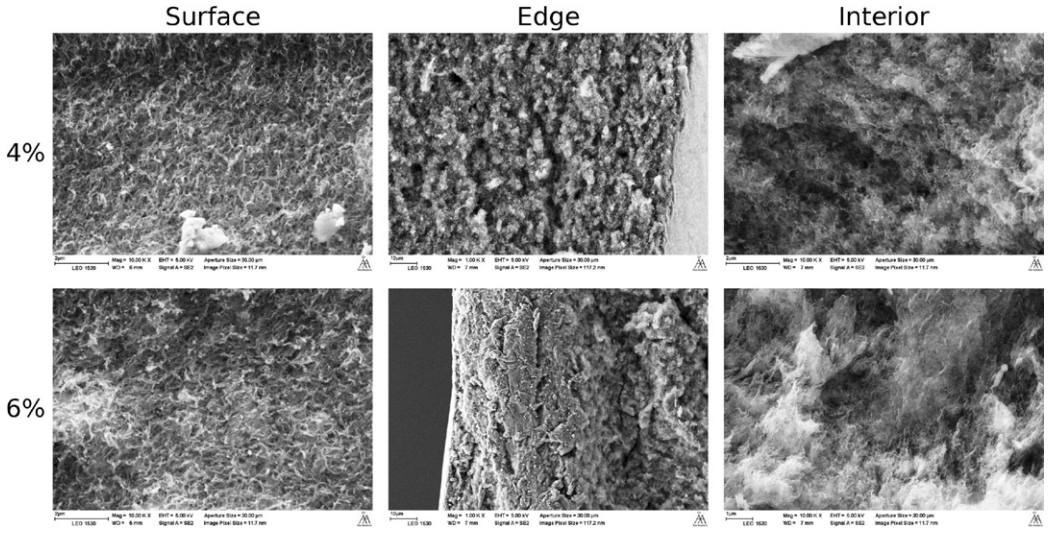

Fig. 6. FE-SEM images of the surface, edge and interior of CPD cellulose beads. 4% and 6% cellulose solution coagulated into 2 M HNO_3 at 25 °C. Magnifications are 1000 (edge) and 10,000× (surface and interior).

bead types resulting from 4% to 6% cellulose solutions. However, in images presenting the edge (Fig. 6, middle) differences under the skin layer were observed. In the interior part, beads, coagulated from 6% cellulose solution, showed more dense structures. Also in images presenting the interior structure (Fig. 6, right) 6% cellulose solution showed smaller pores than 4% solution, as seen in porosity values in Fig. 2C. This can be explained by the similar dimensions of the droplet and coagulated bead with higher amount of cellulose in it (Fig. 2C, volume).

3.4. Surface area

The effect of coagulation bath conditions (medium, temperature and concentration) and cellulose concentration in NaOH–urea–water on specific surface area were studied with CPD beads by nitrogen adsorption method. Increasing the temperature of the coagulation bath from 5 to 50 °C resulted in a decrease of surface area by 15% (2 M acid) and 21% (10% NaCl solution) (Fig. 7A). A decrease of 21% could also be observed when the concentration of the acid increased from 0.5 to 6 M (Fig. 7B). However, a slight increase occurred when 8 and 10 M acid was used. This could be explained by different, competing coagulation mechanism, as mentioned earlier (see Section 3.3). Weakened mechanical stability was observed while handling these beads, indicating less compact structure inside the beads, and hence higher surface area. Weakened structure was not observed when temperature was increased. Apart from 8 to 10 M acid solutions, increasing coagulation kinetics by higher acid concentration or temperature decreased the resulting specific surface area.

After the skin formation, coagulation can be assumed to be mainly diffusion controlled (acid into the beads → neutralization; saline water in and sodium hydroxide and urea out → dilution). Slow diffusion and coagulation arranges cellulose molecules into structures where specific surface area is maximized. When acid concentration was high, higher concentration gradient increased the diffusion rate and neutralization. This increased the kinetics and caused faster agglomeration of cellulose molecules so that they formed denser networks structures.

Beads coagulated from 4% cellulose solution into 2 M acid at 25 °C showed the lowest surface area (Fig. 7C). The difference between 5% and 6% solution was less pronounced. As demonstrated before in Sections 3.2 and 3.3, 6% cellulose solution yielded lower porosity than 4% and 5% solutions (Fig. 2C) because cellulose is packed more densely (Fig. 6).

Adsorption isoterm was measured also for the beads dried at the room temperature for few days. However, the specific surface area was less than one square meter per gram. Evaporized water caused hornification and pores were closed due to high capillary forces.

3.5. Pore size distribution of meso- and macropores

By variation of the coagulation conditions, the effect of the acid concentration (0.5, 2 and 6 M nitric acid at 25 °C) and temperature (2 M acid solution at 5, 25 and 50 °C) on the amount of inaccessible

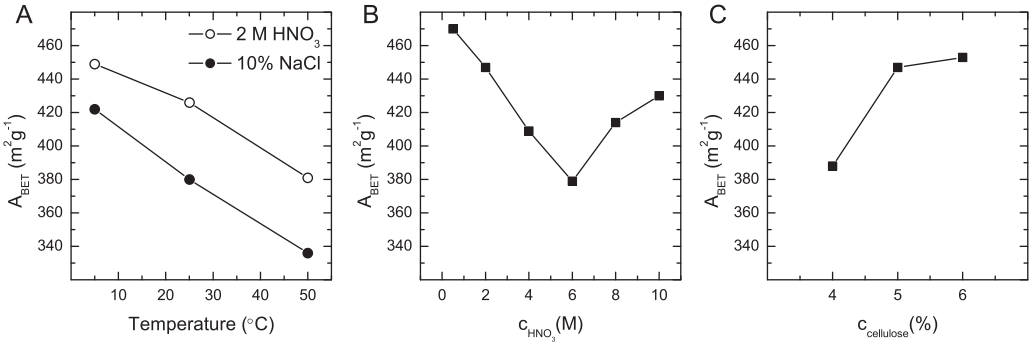

Fig. 7. The effect of (A) temperature, (B) acid concentration and (C) cellulose concentration on specific surface area of the CPD cellulose beads. If not stated otherwise, following coagulation conditions were applied: 5% cellulose solution coagulated into 2 M HNO_3 at 25 °C. Lines are given to guide the eye.

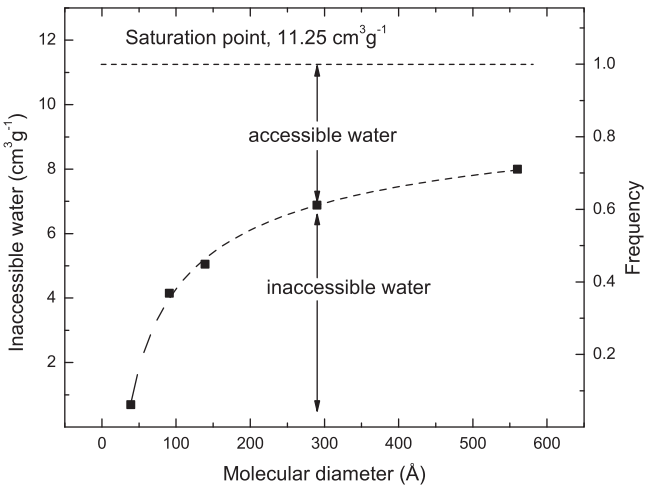

Fig. 8. Inaccessible water, saturation point and frequencies of the pores of the beads coagulated from 5% cellulose solution into 2 M HNO_3 at 25 °C.

water was determined. Total accessible water (saturation point) was computed and relative accessibility (frequency) was calculated for each probe molecule (Fig. 8). Since the total accessible water is related to the dry mass of the beads, total porosity values could be calculated. Porosity varied between 91% and 92% for all samples. Since the values are lower than could be expected from porosity values in Fig. 2A and B, pocket structures and micropores are most likely present where macromolecules cannot access.

When the acid concentration was increased, the presence of macropores (⩾560 Å) was favored over small mesopores (39 Å) (Fig. 9, top). Pores with diameter of 91 Å were more frequent when 0.5 M acid was used but otherwise significant changes were not observed between 139 and 290 Å. Sum of the mesopore frequencies indicates that they are more dominant when acid concentration is low (0.5 M 0.669; 2 M 0.649 and 6 M 0.598). In this case, coagulation was slower and cellulose had more time to arrange itself and form smaller cavities. In contrast, when acid concentration was increased and coagulation was more rapid, more macropores were formed (0.5 M 0.276, 2 M 0.289, and 6 M 0.348). Formation of mesopores seemed to be inversely proportional to the formation of macropores (⩾560 Å). Higher amounts of small pores also explains the higher specific surface area in case of beads coagulated from lower acid concentrations.

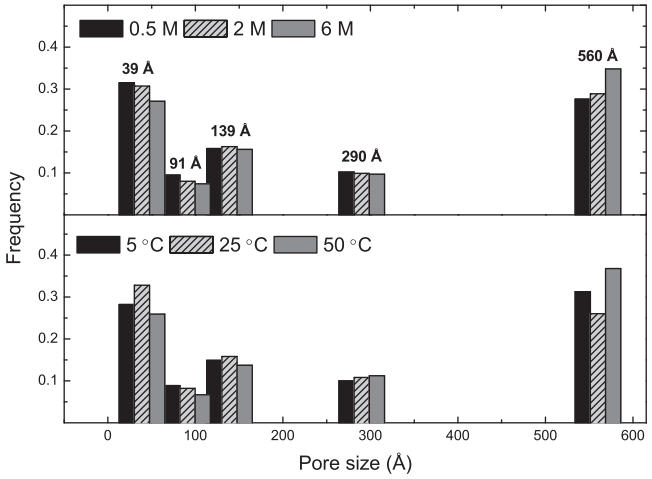

Fig. 9. Pore size distributions of cellulose beads coagulated into (top) 0.5, 2, 6 M HNO_3 at 25 °C and (bottom) 2 M HNO_3 at 5, 25 and 50 °C. Sizes of the employed dextrans are given in top figure.

When beads were coagulated into 2 M acid at various temperatures, coagulation kinetics could not explain all the variations in the pore size distribution. Beads coagulated into 50 °C acid produced more macropores than 25 °C acid (Fig. 9, bottom). In contrast, small mesopores were favored at 25 °C. Similar trends as with macropores were observed in porosity values (Fig. 2A). 25 °C acid produced beads with lower porosity than 5 or 50 °C acid. Since the volume was almost the same at 5 and 25 °C, it could be speculated that faster movement of the cellulose molecules resulted in a decreased amount of macropores and increased amount of mesopores. However, at 50 °C coagulation was rapid enough to freeze the skin layer and volume of the beads increased. This created higher amount of macropores and explains the increased porosity in Fig. 2A.

4. Conclusion

In the present publication, we have demonstrated the preparation of cellulose beads with designed properties using NaOH–urea–water as an environmental friendly polysaccharide solvent. By variation of parameters that effect the coagulation process, in particular temperature (5–50 °C), acid concentration in the coagulation medium (0–10 M) and the cellulose concentration (3–7%), it was possible to tailor volume and weight (8–20 mm^3, 14–22 mg), shape (circularity 0.69–0.89), specific surface area (336–470 $m^2\,g^{-1}$), porosity (93–95%) and pore size distribution.

Based on the results presented it is possible to tune morphology and ultrastructure of cellulose beads. Thus, tailored materials for specific applications such as drug loading or affinity chromatography can be prepared.

Acknowledgements

This work is part of Future Biorefinery (FuBio), funded by TEKES and coordinated by Forest Cluster Oy, Finland.

References

Štamberg, J., Peška, J., Paul, D., & Philipp, B. (1979). Perlcellulose – Ein neuer makroporöser träger für ionenaustauscher und analoge systeme. *Acta Polymerica*, *30*, 734–739.

Brunauer, S., Emmett, P. H., & Teller, E. (1938). Adsorption of gases in multimolecular layers. *Journal of the American Chemical Society*, *60*, 309–319.

Chen, L. F., & Tsao, G. T. (1976). Physical characteristics of porous cellulose beads as supporting material for immobilized enzymes. *Biotechnology and Bioengineering*, *18*, 1507–1516.

Cuissinat, C., & Navard, P. (2006). Swelling and dissolution of cellulose. Part II: Free floating cotton and wood fibres in NaOH–water–additives systems. *Macromolecular Symposia*, *244*, 19–30.

De Oliveira, W., & Glasser, W. G. (1996). Hydrogels from polysaccharides. I. Cellulose beads for chromatographic support. *Journal of Applied Polymer Science*, *60*, 63–73.

Domsjö (2007). *Specification Domsjö cellulose*. http://www.domsjoe.com – Produkter – Specialcellulosa – Produktinformation Domsjö Cellulose. Accessed 10.11.10.

Egal, M., Budtova, T., & Navard, P. (2008). The dissolution of microcrystalline cellulose in sodium hydroxide–urea aqueous solutions. *Cellulose*, *15*, 361–370.

Ettenauer, M., Loth, F., Thümmler, K., Fischer, S., Weber, V., & Falkenhagen, D. (2011). Characterization and functionalization of cellulose microbeads for extracorporeal blood purification. *Cellulose*, *18*, 1257–1263.

Gavillon, R., & Budtova, T. (2008). Aerocellulose: New highly porous cellulose prepared from cellulose–NaOH aqueous solutions. *Biomacromolecules*, *9*, 269–277.

Heinze, T., Liebert, T., & Koschella, A. (2006). *Esterification of polysaccharides*. Berlin, Heidelberg: Springer.

Hirota, M., Tamura, N., Saito, T., & Isogai, A. (2009). Surface carboxylation of porous regenerated cellulose beads by 4-acetamide-TEMPO/NaClO/$NaClO_2$ system. *Cellulose*, *16*, 841–851.

Immergut, E., Schurz, J., & Mark, H. (1953). Viskositätszahl-molekulargewichtsbeziehung für cellulose und untersuchungen von nitrocellulose in verschiedenen lösungsmitteln. *Monatshefte fur Chemie*, *84*, 219–249.

Jin, H., Zha, C., & Gu, L. (2007). Direct dissolution of cellulose in NaOH/thiourea/urea aqueous solution. *Carbohydrate Research*, *342*, 851–858.

Kaster, J. A., de Oliveira, W., Glasser, W. G., & Velander, W. H. (1993). Optimization of pressure-flow limits, strength, intraparticle transport and dynamic capacity by hydrogel solids content and bead size in cellulose immunosorbents. *Journal of Chromatography A*, *648*, 79–90.

Klemm, D., Philipp, B., Heinze, T., Heinze, U., & Wagenknecht, W. (1998). *Comprehensive cellulose chemistry: Functionalization of cellulose*. Weinheim: Wiley-VCH.
Lönnberg, B. (2005). *New development in cellulose technology. Polysaccharides – Structural diversity and functional versatility* (2nd ed.). New York: Marcel Dekker.
Liebert, T. F., Heinze, T. J., & Edgar, K. J. (Eds.). (2010). *Cellulose solvents: For analysis, shaping and chemical modification (Vol. 1033)*. American Chemical Society.
Liu, W., Budtova, T., & Navard, P. (2011). Influence of ZnO on the properties of dilute and semi-dilute cellulose–NaOH–water solutions. *Cellulose*, *18*, 911–920.
Luo, X., & Zhang, L. (2010). Creation of regenerated cellulose microspheres with diameter ranging from micron to millimeter for chromatography applications. *Journal of Chromatography A*, *1217*, 5922–5929.
Motozato, Y., & Hirayama, C. (1984). Preparation and properties of cellulose spherical particles and their ion exchangers. *Journal of Chromatography A*, *298*, 499–507.
Motozato, Y., & Ishibashi, H. (1981). Process for preparing porous cellulose spherical particles. *Eur. Pat. App.*,. EP0025639
Origin Software. (2002). *Version 7.0*. Northampton, MA, USA: OriginLab Corporation.
Peška, J., Štamberg, J., & Hradil, J. (1976). Chemical transformations of polymers. XIX. Ion exchange derivatives of bead cellulose. *Die Angewandte Makromolekulare Chemie*, *53*, 73–80.
Peška, J., Štamberg, J. & Blace, Z., (1977). Method for manufacturing of spherical cellulose particles. United States Patent 4,055,510.
Pinnow, M., Fink, H.-P., Fanter, C., & Kunze, J. (2008). Characterization of highly porous materials from cellulose carbamate. *Macromolecular Symposia*, *262*, 129–139.
Rosenberg, P., Suominen, I., Rom, M., Janicki, J., & Fardim, P. (2007). Tailored cellulose beads for novel applications. *Cellulose Chemistry and Technology*, *41*, 243–254.
Rosenberg, P., Rom, M., Janicki, J., & Fardim, P. (2008). New cellulose beads from biocelsol solution. *Cellulose Chemistry and Technology*, *42*, 293–305.
Schindelin, J. (2008). Fiji is just ImageJ (batteries included). version 1.44. In *ImageJ User and Developer Conference* .
Sescousse, R., Gavillon, R., & Budtova, T. (2011). Wet and dry highly porous cellulose beads from cellulose–NaOH–water solutions: Influence of the preparation conditions on beads shape and encapsulation of inorganic particles. *Journal of Materials Science*, *46*, 759–765.
Stone, J., & Scallan, A. (1967). The effect of component removal upon the porous structure of the cell wall of wood. II. Swelling in water and the fiber saturation point. *Tappi*, *50*, 496–501.
Stone, J., & Scallan, A. (1968). A structural model for the cell wall of water–swollen wood pulp fibres based on their accessibility to macromolecules. *Cellulose Chemistry and Technology*, *2*, 343–358.
Thümmler, K., Fischer, S., Feldner, A., Weber, V., Ettenauer, M., Loth, F., & Falkenhagen, D. (2011). Preparation and characterization of cellulose microspheres. *Cellulose*, *18*, 135–142.
Trygg, J., & Fardim, P. (2011). Enhancement of cellulose dissolution in water-based solvent via ethanol–hydrochloric acid pretreatment. *Cellulose*, *18*, 987–994.
Volkert, B., Wolf, B., Fischer, S., Li, N., & Lou, C. (2009). Application of modified bead cellulose as a carrier of active ingredients. *Macromolecular Symposia*, *280*, 130–135.
Wolf, B. (1997). Bead cellulose products with film formers and solubilizers for controlled drug release. *International Journal of Pharmaceutics*, *156*, 97–107.
Xia, H.-F., Lin, D.-Q., Wang, L.-P., Chen, Z.-J., & Yao, S.-J. (2008). Preparation and evaluation of cellulose adsorbents for hydrophobic charge induction chromatography. *Industrial & Engineering Chemistry Research*, *47*, 9566–9572.
Yamamoto, S., & Miyagawa, E. (1999). Retention behavior of very large biomolecules in ion-exchange chromatography. *Journal of Chromatography A*, *852*, 25–30.
Zhang, L., Ruan, D., & Gao, S. (2002). Dissolution and regeneration of cellulose in NaOH/thiourea aqueous solution. *Journal of Polymer Science. Part B: Polymer Physics*, *40*, 1521–1529.